Solar Energy Materials & Solar Cells 120 (2014) 436–440

Contents lists available at ScienceDirect

Solar Energy Materials & Solar Cells

journal homepage: www.elsevier.com/locate/solmat

Injection dependence of the effective lifetime of *n*-type Si passivated by Al_2O_3: An edge effect?

Boris Veith [a,*], Tobias Ohrdes [a], Florian Werner [a], Rolf Brendel [a,b], Pietro P. Altermatt [a,b], Nils-Peter Harder [a,c], Jan Schmidt [a,b]

[a] Institute for Solar Energy Research Hamelin (ISFH), Am Ohrberg 1, 31860 Emmerthal, Germany
[b] Institute of Solid-State Physics, Leibniz Universität Hannover, Appelstrasse 2, 30167 Hannover, Germany
[c] Institut für Materialien und Bauelemente der Elektronik, Leibniz Universität Hannover, Schneiderberg 32, 30167 Hannover, Germany

ARTICLE INFO

Available online 3 August 2013

Keywords:
Aluminum oxide
Silicon
Charge carrier lifetime
Modeling
Surface passivation

ABSTRACT

Aluminum oxide provides an excellent surface passivation on *p*- and *n*-type crystalline silicon. On *n*-type silicon, however, the effective excess carrier lifetime τ_{eff} is often found to be injection dependent. Our experimental results show that, in our case, this effect depends mainly on the size of the lifetime samples. The fixed negative charges present at the Al_2O_3/c-Si interface induce an inversion layer at the surface, which results in a *p*–*n*-junction close to the surface of the sample and the inversion layer couples the sensing area with the poorly passivated or damaged edge of the sample. For smaller samples stronger injection-dependent lifetimes are measured, whereas large samples show a smaller injection dependence. In addition, photoconductance-calibrated photoluminescence lifetime images show that for low injection levels the lifetime decreases towards the sample edge. Device simulations for different sample sizes including the edge recombination are in agreement with the measured injection-dependent lifetimes. Therefore, it is necessary to use sufficiently large samples or decouple the sensing area form the edge when evaluating the injection dependence of the lifetime. For the samples used in this contribution, the injection dependence of the lifetime did not even fully vanish for an edge length of 12.5 cm.

1. Introduction

In recent years, aluminum oxide (Al_2O_3) has proven to provide an excellent surface passivation for both *p*- and *n*-type silicon wafers [1,2]. On *p*-type silicon, this surface passivation was shown to be independent of the excess carrier density Δn at low injection levels. However, for *n*-type silicon wafers passivated with Al_2O_3 the effective excess carrier lifetime τ_{eff} was found to depend on Δn at low injection levels [3,4]. When applied to a solar cell, this would result in a reduced conversion efficiency under weak light conditions [5]. As a consequence, Al_2O_3 is often considered as an excellent passivation layer on *p*-type silicon showing a reduced passivation on *n*-type silicon surfaces. For the injection dependence of the effective lifetime measured on Al_2O_3-passivated *n*-type silicon samples, two hypothetical explanations have been published in the recent literature [6,7]. It was conjectured that one reason might be an asymmetric capture cross section of the holes and electrons at the Al_2O_3/Si interface; however, the measured capture cross sections are not asymmetric enough to explain the measured injection dependence [6]. Another proposed explanation was that a damaged region in the silicon bulk close to the interface is causing the pronounced $\tau_{eff}(\Delta n)$ dependence. So far, however, no unambiguous experimental validation could be found for the existence of this damaged region. Recently, Kessler et al. [8] gave a different explanation for injection-dependent lifetimes of *n*-type Si samples with boron-diffused p^+-emitters. They showed that the injection dependence measured on these samples resulted partly from edge recombination of the samples and is therefore dependent on the sample size. In the present work, we evaluate if a similar effect might explain the pronounced $\tau_{eff}(\Delta n)$ dependence measured on Al_2O_3-passivated *n*-type silicon samples, where a hole-conducting inversion layer due to the fixed negative charge density in the Al_2O_3 is present instead of a diffused p^+-emitter. This effect could – at least partly – also be the reason for the pronounced $\tau_{eff}(\Delta n)$ dependence typically measured on *p*-type silicon samples passivated with SiN_x, which is known to contain a high density of fixed positive charges. Edge recombination effects have already been identified as reason for a reduction in the open-circuit-voltage (V_{oc}) and fill factor (*FF*) of various types of solar cells [9,10].

2. Experimental details

Lifetime test samples are fabricated on *p*- and *n*-type float-zone (FZ) silicon wafers with a resistivity of 1.4 Ω cm and 1.2 Ω cm,

* Corresponding author. Tel.: +49 5151 999 635; fax: +49 5151 999 400.
E-mail address: b.veith@isfh.de (B. Veith).

0927-0248/$ - see front matter © 2013 Elsevier B.V. All rights reserved.
http://dx.doi.org/10.1016/j.solmat.2013.06.049

respectively. The samples are laser-cut into 12.5×12.5 cm^2 pseudo-square or 6×6 cm^2, 4×4 cm^2, and 2.5×2.5 cm^2 full-square samples. All samples are KOH-etched in order to remove the laser damage and are subsequently RCA-cleaned. After KOH etching, the wafers have a thickness of 260 μm. On both sides of the samples, a 15 nm thick Al_2O_3 layer is deposited using plasma-assisted atomic layer deposition (PA ALD) in a FlexAL™ reactor [11] (Oxford Instruments). After Al_2O_3 deposition the samples are annealed at 425 °C for 15 min in a nitrogen ambient to activate the Al_2O_3 passivation. The samples are characterized using the photoconductance decay (PCD) method [12] (Sinton Instruments WCT120 lifetime tester in the transient mode). In order to reduce the possible impact of stray light, a black box is placed on top of the setup. After PCD measurement, some of the 12.5×12.5 cm^2 pseudo-square samples are laser cut into 6 cm, 4 cm and 2.5 cm wide stripes and are measured again. In order to measure the spatial distribution of the effective lifetime, we apply photoconductance-calibrated photoluminescence lifetime imaging (PC-PLI) [13] to some selected samples. In order to model the influence of the edge recombination, two-dimensional simulations of quasi-steady-state photoconductance (QSSPC) measurements were performed using Sentaurus device [14] using modeling parameters described by Altermatt [15].

3. Experimental results

Fig. 1(a) shows the effective carrier lifetime τ_{eff} measured using PCD as a function of excess carrier density Δn. It can be seen that some of the Al_2O_3-passivated n-type Si samples show a pronounced injection dependence of the effective carrier lifetime. The 12.5×12.5 cm^2 sample shows only negligible injection dependence, whereas the 4×4 cm^2 sample shows the most pronounced dependence. For the 2.5×2.5 cm^2 sample an overall lower lifetime is measured, which we partly attribute to a measurement artifact, as the sample might be smaller than the sensing area of the Sinton Instruments lifetime tester. The samples that were laser cut after Al_2O_3 deposition show the same injection and sample size dependence. This finding is consistent with a poorly passivated or damaged edge region. The damage induced by the laser cutting might not have been removed by the KOH etching step or the KOH etch itself introduced a damage. It is also possible that the Al_2O_3 layer could not passivate the edge effectively. However, due to the depletion region modulation (DRM) effect [16] no information about the injection dependence can be obtained for injection densities below $\Delta n = 4 \times 10^{13}$ cm^{-3} and for the large sample even below $\Delta n = 1 \times 10^{14}$ cm^{-3}. It has to be noted that the DRM effect shifts towards lower injection densities when the setup is not shielded from the surrounding room light. The lifetimes of the p-type samples also show some injection dependence. The reason for this behavior is not fully understood, however, injection-dependent lifetimes on Al_2O_3-passivated p-type silicon wafers have also been reported in the literature [2,17,18]. In our case it might be due to some contamination of the p-type samples, such as iron, or due to a damaged region close to the surface [7] maybe introduced by the KOH etch itself. However, we observe no systematic impact of the sample size on the injection dependence. Only the overall lifetime for the 12.5×12.5 cm^2 p-type sample is reduced. Therefore, the lifetime measurements depend on the sample size only for the n-type samples. To obtain more information on the spatial distribution of the effective lifetime and the behavior in the low-injection range, some of the samples were measured using the PC-PLI method. Fig. 1(b) shows the effective lifetime of the samples extracted from PC-PLI measurements as a function of excess carrier density. Shown are area averages, with the area size chosen to fit the approximate detection region of the PCD measurement in (a). The effective carrier lifetime of the n-type samples is – with exception of the 2.5×2.5 cm^2 sample – the same as measured with PCD, except that no DRM effect can be observed. The PC-PLI measurement shows a more pronounced injection dependence for the 2.5×2.5 cm^2 sample, leading to a comparable $\tau_{eff}(\Delta n)$ dependence for the 2.5×2.5 cm^2 and 4×4 cm^2 samples and also for the 6×6 cm^2 sample at lower injection densities. The effective carrier lifetimes of the p-type samples show almost no injection dependence in the PC-PLI measurements. In conclusion, the PC-PLI data exhibit a strong difference between the injection dependence of p- and n-type samples. On p-type silicon, the lifetimes change only by a factor of 2 over a wide injection range, whereas the lifetimes of the n-type silicon samples change by one order of magnitude over the measured injection range.

Fig. 2(a) shows a PC-PL image of a 12.5×12.5 cm^2 Al_2O_3-passivated n-type Si sample. In the center of the sample the lifetime is around 9 ms, with the exception of a spot which probably results from the cleaning procedure. Closer to the edge the lifetime strongly decreases. This can be seen quantitatively in Fig. 2(b), where the lifetime as a function of excess carrier density is extracted from the PC-PL images in the marked regions in Fig. 2(a). The injection dependence at the three marked regions 2–4 close to the edge is similar. The lifetime of the marked region 1 close to the center shows the same injection dependence for $\Delta n < 1 \times 10^{13}$ cm^{-3}

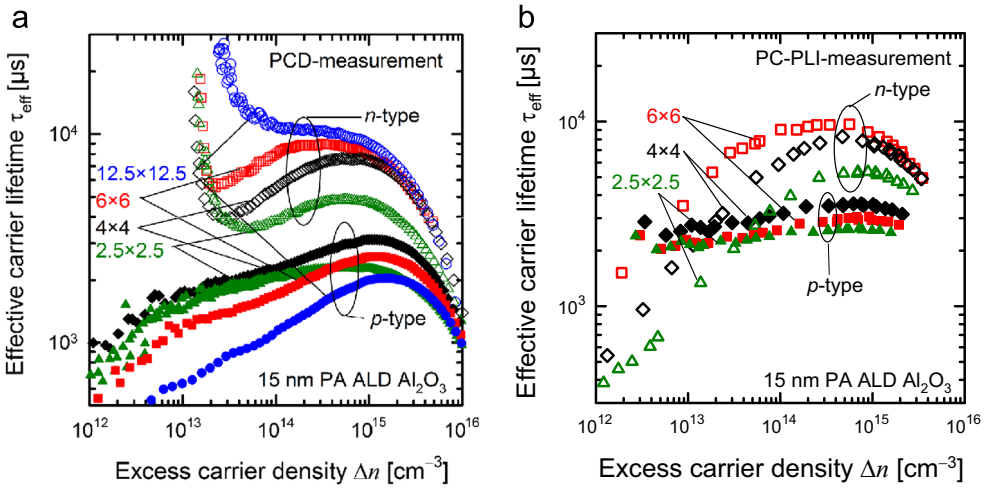

Fig. 1 (Color online). Effective carrier lifetime τ_{eff} as a function of excess carrier density Δn of Al_2O_3-passivated 1.2 Ω cm n-type and 1.4 Ω cm p-type FZ-Si wafers of different sample sizes. (a) PCD measurements, (b) PC-PLI measurements.

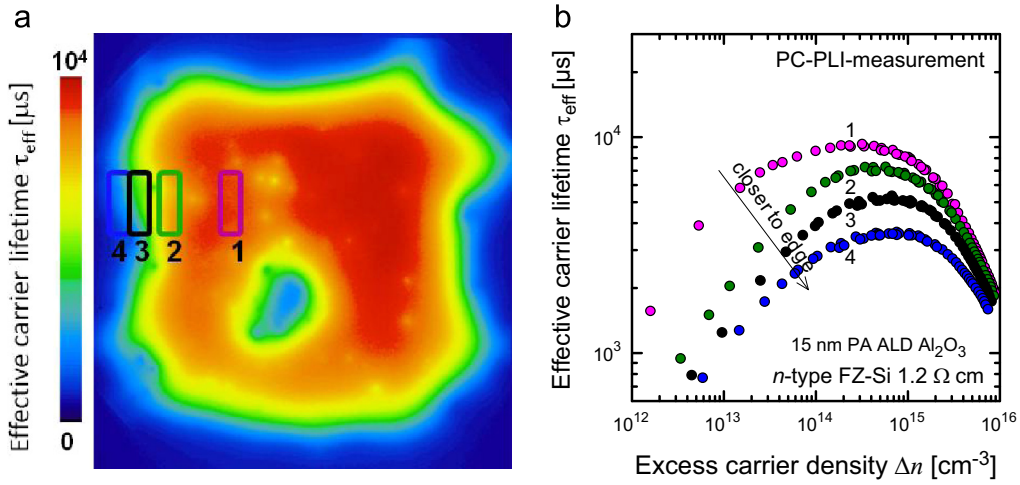

Fig. 2 (Color online). (a) PC-PL image of a 12.5×12.5 cm^2 Al_2O_3-passivated n-type Si sample. The excess carrier density is between 4×10^{12} and 4×10^{13} cm^{-3}. (b) Extracted carrier lifetime as a function of excess carrier density. The lifetimes are averaged over the marked areas in (a).

but in comparison with the regions 2–4 this injection dependence starts at lower injection densities. This behavior is comparable to the 6×6 cm^2 sample. It is important to note that the lifetime around the poorly passivated spot close to the center of Fig. 2(a) is reduced and shows a stronger injection dependence, therefore the data of the 12.5×12.5 cm^2 sample have not been included in Fig. 1 (b).

These experimental findings lead to the conclusion that the sample edges, or other poorly passivated regions, have a significant influence on the injection dependence of the effective lifetime. The effective lifetime is not only reduced at the edges themselves, but also up to several centimeters into the samples. This results not only in different injection dependences for samples of different sizes but can also reduce the overall lifetime, as observed for the PCD measurements on the 2.5×2.5 cm^2 samples and the PC-PLI measurements on the large-area sample.

4. Two-dimensional modeling

The simulation domain of our Sentaurus [14] simulations is shown in Fig. 3. Corresponding to the Al_2O_3 passivation of our samples, a fixed charge density of $Q_f = -4 \times 10^{12}$ cm^{-2} was assumed. The surface recombination velocity (SRV) parameters $S_{n0} = S_{p0} = 200$ cm/s were chosen to fit the measured $\tau_{eff}(\Delta n)$ curves. At the edge of the sample, the SRV is set at $S_{edge} = 1 \times 10^5$ cm/s to account for a damage created by the laser cutting or/and a poor surface passivation quality. The electron and hole lifetimes of the silicon substrate are set at $\tau_{n0} = \tau_{p0} = 30$ ms. The excess carrier density Δn is determined in a 2 cm wide area in the middle of the sample, which represents the sensing area of the coil in the lifetime tester.

QSSPC simulations based on this model were performed for different sample sizes for both n- and p-type silicon substrates. The resulting lifetime data as a function of excess carrier density is shown in Fig. 4 as lines. The simulations of n-type samples, different to the p-type samples, show injection dependent lifetimes that depend on the sample size and are in agreement with the measured $\tau_{eff}(\Delta n)$ curves.

In order to fully understand the physics behind the measured effects, the limiting factors for the local recombination rate at the edges have to be identified. Kessler et al. [8] showed that the injection-dependent lifetime can be explained by the high SRH recombination rate at the edge and the carrier transport to the edge. The transport of charge carriers towards the location of

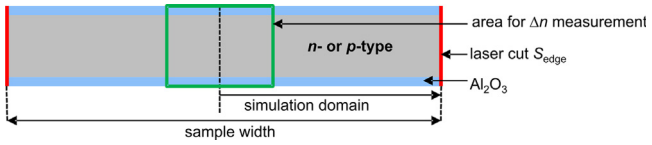

Fig. 3 (Color online). Sentauraus simulation domain for QSSPC lifetime simulations. The area in the middle of the sample marked with a (green) box represents the sensing area of the lifetime tester.

recombination is a crucial parameter because it is able to limit the recombination rate: In the case of an n-type silicon sample without an inversion layer, the recombination at the edge is limited by the diffusion of holes towards the edge. The diffusion length of holes in our samples is about 3 mm. Therefore, the recombination at the edge does not influence the charge carrier density in the sensing area very much and no injection dependence is observed (see Fig. 4(b) for the case of electron transport in a p-type sample). In case of a sample with an inversion layer, the limitation of the transport towards the edge changes for different injection levels. As a reason for this behavior two important mechanisms can be found: (i) The main transport mechanism of majority charge carriers in the n-type base is drift. The p-type inversion layer enables the drift transport of holes. This results in a good transport of both carrier types towards the edge, even for a distance of several centimeters and causes the low lifetime at low injection levels in the entire sample. (ii) At the poorly passivated or/and damaged sample edge, the excess carriers recombine through surface states mainly in the region of the edge surface where minority and majority carrier concentrations are approximately equal due to the depletion region. The high recombination rate at the edge results in an inhomogeneous charge carrier distribution from the middle of the sample to the edge. This is equivalent to a voltage drop of the electrostatic potential at the edge. As shown in Fig. 5, the voltage drop towards the sample edge increases and becomes steeper (i.e. the electric field increases) with increasing excess carrier concentration due to an increased recombination rate. However, towards the center only a small difference in electrostatic potential is observed and this limits the drift of majority charge carriers in the inversion layer towards the edge. This results in an almost constant transport of charge carriers through the inversion layer to the recombination center at the edge over the injection density range and therefore an injection-dependent lifetime in the sample. Therefore, the

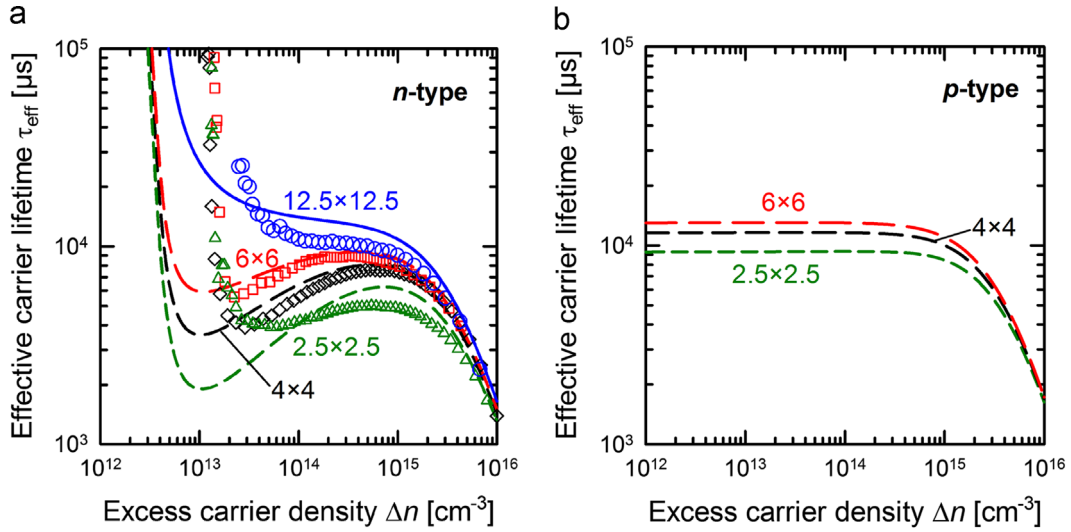

Fig. 4 (Color online). Simulated lifetimes (lines) and measured lifetimes (symbols) as a function of excess carrier density on (a) *n*-type and (b) *p*-type c-Si passivated by Al_2O_3.

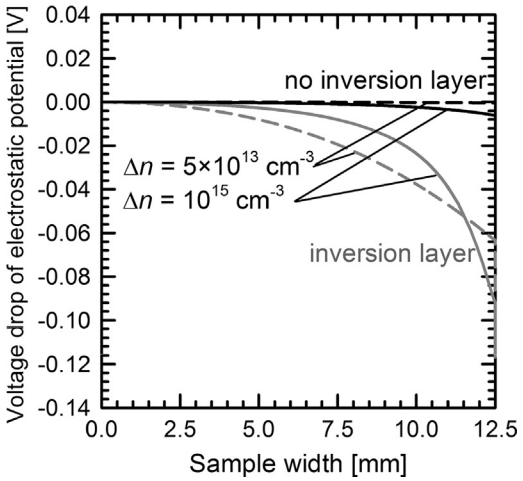

Fig. 5. Voltage drop of the electrostatic potential along the sample width in the inversion layer (or very close to the surface in case no inversion layer is present) of a $2.5 \times 2.5\ cm^2$ sample. In the sample with inversion layer the electrostatic potential shows a steeper and larger decline at an excess carrier concentration of $\Delta n = 10^{15}\ cm^{-3}$ (solid lines) compared to $\Delta n = 5 \times 10^{13}\ cm^{-3}$ (dashed lines). The voltage drop in the sample without inversion layer is smaller and only visible within a distance of the diffusion length of holes (approx. 3 mm) to the edge.

injection dependence of the lifetime is a result of a limited carrier drift towards the edge.

Our simulations show that the pronounced injection dependence of the lifetime measured on Al_2O_3-passivated *n*-type silicon samples can be explained by assuming a poorly passivated and/or damaged sample edge and that asymmetric capture cross sections at the Al_2O_3/Si interface or a damaged region at the silicon surface underneath the Al_2O_3 layer are both not necessary to explain the pronounced injection dependence frequently measured on Al_2O_3-passivated *n*-type silicon wafers. In general, this leads to the conclusion that a poorly passivated localized area on the sample surface or a locally reduced bulk lifetime in the silicon material result in an injection-dependent lifetime of the Al_2O_3-passivated *n*-type silicon sample (or the SiN_x-passivated *p*-type silicon sample) even in a distance of several centimeters of the local spot of increased recombination. Our simulations further show that this effect is more pronounced for samples with higher carrier lifetimes.

5. Conclusions

Our experiments showed a pronounced dependence of the carrier lifetime measured on Al_2O_3-passivated *n*-type silicon wafers on the sample size. Interestingly, the larger the samples the weaker was the injection dependence. Therefore, we conclude that the injection dependence in our samples is not mainly caused by near-surface damage of the silicon underneath the Al_2O_3 layer, as was conjectured in previous studies [6,7]. In addition, our photoluminescence lifetime images showed a reduced lifetime towards the edges of the wafers and a more pronounced injection dependence of the effective lifetime close to the sample edges.

We were able to simulate the measured $\tau_{eff}(\Delta n)$ dependences using only the assumption of an increased recombination at the sample edge. The high recombination rate at the edge and the transport of holes through the inversion layer induced by the fixed negative charges in the Al_2O_3 film affects the injection dependence of the lifetime within the sensing area of the lifetime measurement, even up to a sample edge length of 12.5 cm. The same conclusion should also hold true for the injection dependence of SiN_x-passivated *p*-type silicon samples. Therefore, we conclude that it is important to avoid the influence of the edge when measuring the injection dependence of the effective lifetime, either by decoupling the edge from the sensing area or by using samples with a sufficiently large size. The higher the lifetime of a silicon wafer the larger needs to be the sample size.

Acknowledgments

The authors thank M. Kessler for fruitful discussions. Funding was provided by the State of Lower Saxony and the German Ministry for the Environment, Nature Conservation and Nuclear Safety (BMU) under Contract no. 0325050 (“ALD”).

References

[1] G. Agostinelli, A. Delabie, P. Vitanov, Z. Alexieva, H.F.W. Dekkers, S. De Wolf, G. Beaucarne, Very low surface recombination velocities on p-type silicon wafers passivated with a dielectric with fixed negative charge, Solar Energy Materials and Solar Cells 90 (2006) 3438–3443.

[2] B. Hoex, S.B.S. Heil, E. Langereis, M.C.M. van de Sanden, W.M.M. Kessels, Ultralow surface recombination of c-Si substrates passivated by plasma-

assisted atomic layer deposited Al_2O_3, Applied Physics Letters 89 (2006) 042112-1–042112-3.
[3] B. Hoex, J. Schmidt, P. Pohl, M.C.M. van de Sanden, W.M.M. Kessels, Silicon surface passivation by atomic layer deposited Al_2O_3, Journal of Applied Physics 104 (2008) 044903-1–044903-12.
[4] G. Dingemans, N.M. Terlinden, M.A. Verheijen, M.C.M. van de Sanden, W.M.M. Kessels, Controlling the fixed charge and passivation properties of Si (100)/Al_2O_3 interfaces using ultrathin SiO_2 interlayers synthesized by atomic layer deposition, Journal of Applied Physics 110 (2011) 093715-1–093715-6.
[5] B. Vermang, E. Cornagliotti, V. Prajapati, J. John, J. Poortmans, R. Mertens, Assessment of the illumination dependency of Al_2O_3 and SiO_2 rear-passivated p-type silicon solar cells, Physica Status Solidi RRL 6 (2012) 259–261.
[6] F. Werner, A. Cosceev, J. Schmidt, Interface recombination parameters of atomic-layer-deposited Al_2O_3 on crystalline silicon, Journal of Applied Physics 111 (2012) 073710-1–073710-6.
[7] F.-J. Ma, G.G. Samudra, M. Peters, A.G. Aberle, F. Werner, J. Schmidt, B. Hoex, Advanced modeling of the effective minority carrier lifetime of passivated crystalline silicon wafers, Journal of Applied Physics 112 (2012) 054508-1–054508-8.
[8] M. Kessler, T. Ohrdes, P.P. Altermatt, R. Brendel, The effect of sample edge recombination on the averaged injection-dependent carrier lifetime in silicon, Journal of Applied Physics 111 (2012) 054508-1–054508-12.
[9] D. König, D. Ebest, New contact frame design for minimizing losses due to edge recombination and grid-induced shading, Solar Energy Materials and Solar Cells 75 (2003) 381–386.
[10] K.R. McIntosh, C.B. Honsberg, The influence of edge recombination on a solar cell's *IV* curve, in: Proceedings of the 16th PVSEC, Glasgow, UK, 2000, pp. 1651–1654.
[11] S.B.S. Heil, J.L. van Hemmen, C.J. Hodson, N. Singh, J.H. Klootwijk, F. Roozeboom, et al., Deposition of TiN and HfO_2 in a commercial 200 mm remote plasma atomic layer deposition reactor, Journal of Vacuum Science and Technology 25 (2007) 1357–1366.
[12] D.E. Kane, R.M. Swanson, Measurement of the emitter saturation current by a contactless photoconductivity decay method, in: Proceedings of the 18th IEEE Photovoltaic Specialists Conference, Las Vegas, USA, 1985, pp. 578–583.
[13] S. Herlufsen, J. Schmidt, D. Hinken, K. Bothe, R. Brendel, Photoconductance-calibrated photoluminescence lifetime imaging of crystalline silicon, Physica Status Solidi Rapid Research Letters 2 (2008) 245–247.
[14] Sentaurus Device User Guide, Version C-2009.06, Synopsys, Inc., Mountain View, CA.
[15] P.P. Altermatt, Models for numerical device simulations of crystalline silicon solar cells – a review, Journal of Computational Electronics 10 (2011) 314–330.
[16] P.J. Cousins, D.H. Neuhaus, J.E. Cotter, Experimental verification of the effect of depletion-region modulation on photoconductance lifetime measurements, Journal of Applied Physics 95 (2004) 1854–1858.
[17] J. Benick, A. Richter, M. Hermle, S.W. Glunz, Thermal stability of the Al_2O_3 passivation on p-type silicon surfaces for solar cell applications, Physica Status Solidi RRL 3 (2009) 233–235.
[18] P. Saint-Cast, D. Kania, M. Hofmann, J. Benick, J. Rentsch, R. Preu, Very low surface recombination velocity on p-type c-Si by high-rate plasma-deposited aluminum oxide, Applied Physics Letters 95 (2009) 151502-1–151502-3.